

Electronic and magnetic properties of V-doped anatase TiO₂ from first principles

Xiaosong Du,¹ Qunxiang Li,^{1,*} Haibin Su,² and Jinlong Yang¹

¹*Hefei National Laboratory for Physical Sciences at Microscale, University of Science and Technology of China, Hefei, Anhui 230026, P.R. China*

²*School of Materials Science and Engineering, Nanyang Technological University, 50 Nanyang Avenue, 639798, Singapore*

Abstract

We report a first-principles study on the geometric, electronic and magnetic properties of V-doped anatase TiO₂. The DFT+U (Hubbard coefficient) approach predicts semiconductor band structures for Ti_{1-x}V_xO₂ (x=6.25 and 12.5 %), in good agreement with the poor conductivity of samples, while the standard calculation within generalized gradient approximation fails. Theoretical results show that V atoms tend to stay close and result in strong ferromagnetism through superexchange interactions. Oxygen vacancy induced magnetic polaron could produce long-range ferromagnetic interaction between largely separated magnetic impurities. The experimentally observed ferromagnetism in V-doped anatase TiO₂ at room temperature may originate from a combination of short-range superexchange coupling and long-range bound magnetic polaron percolation.

*Corresponding author. E-mail: liqun@ustc.edu.cn

The discovery of ferromagnetism (FM) in Co-containing TiO₂ semiconductors has attracted significant attention because of its potential application for developing functional devices that manipulate both spin and charge.[1] However, the origin of FM observed in Co-doped anatase TiO₂ at and above room temperature is still under debate.[2] Many experiments argued the intrinsic nature of FM, [3, 4, 5] while the presence of the Co clusters in the samples could not be completely excluded.[6, 7] To study the observed FM, theoretical efforts have been made through analyzing the electronic and magnetic structures for various Co configurations in the host matrix. Yang *et al.* have pointed out that ferromagnetic ordering occurs only when Co atoms locate close to each other.[8] One plane-wave pseudopotential calculation supports that the short-range exchange between adjacent Co atoms could contribute to FM.[9] In addition, oxygen vacancy is shown to play a key role in enhancing the FM coupling.[10, 11, 12] Recently, V-doped anatase TiO₂ has been discovered to have a surprisingly high Curie temperature ($T_C > 400$ K).[13] In contrast to Co-doped TiO₂ that has been widely studied theoretically, few investigations on V-doped TiO₂ have been reported in the literature. One interesting work by Wang *et al.* using LDA and LDA+U methods investigates the electronic structure of Ti_{1-x}V_xO₂ (x=6.25%) and argues that the neighboring V-V cations prefers FM at a high doping concentration (x=25%) by employing a 2×1×1 supercell.[14] However, the relative stability among magnetic phases is extremely sensitive to atomistic structure, its associated defects' distribution and dopant concentration, further investigation is desirable to gain better understanding of high T_C FM in this system.

In this paper, we use *ab initio* band-structure and total energy methods, implemented in the Vienna *Ab initio* Simulation Package (VASP),[15, 16] to study the geometric, electronic and magnetic properties of V-doped anatase TiO₂ (Ti_{1-x}V_xO₂), in particular the effects of doping concentration (x=6.25% and 12.5%) as well as oxygen vacancy. The projector augmented wave (PAW) method is chosen to represent the electron-ion interaction.[15] Exchange correlation interactions are described by the Perdew-Burke-Ernzerhof generalized gradient approximation (GGA).[17] The Brillouin-zone (BZ) integration is performed on a well converged Monkhost-Pack k-points grid[18]. The plane wave kinetic energy cutoff is set to be 400 eV. Atomic positions and lattice parameters are optimized at GGA level until the atomic forces are smaller than 0.01 eV/Å. To account for the strongly correlated interactions of the V 3d electrons, a moderate on-site Coulomb repulsion (U=3.0 eV) has been applied

only to V $3d$ orbitals since further correction for the host material has little impact on the magnetic ordering.[19]

We start with a $\text{Ti}_{15}\text{VO}_{32}$ supercell to model the low doping concentration case (6.25%), where a 48-atom $2\times 2\times 1$ supercell of pure anatase TiO_2 ($\text{Ti}_{16}\text{O}_{32}$) is demonstrated in Fig.1 and one V atom substitutes Ti at Ti_1 site. The lattice parameters of optimized $\text{Ti}_{15}\text{VO}_{32}$ supercell are $a=7.64$ Å and $c=9.65$ Å, which are slightly smaller than those of perfect TiO_2 (our theoretical lattice parameters of $\text{Ti}_{16}\text{O}_{32}$ are $a=7.65$ Å and $c=9.68$ Å at GGA level). Clearly, this type of substitution only leads to a small geometrical distortion in the vicinity of V impurity (less than 0.1 Å). To discuss the solubility of V in anatase TiO_2 host, it is useful to define the substitution energy of V impurity as $E_s=E(\text{Ti}_{15}\text{VO}_{32})+E(\text{Ti})-E(\text{V})-E(\text{Ti}_{16}\text{O}_{32})$, where $E(\text{Ti}_{16}\text{O}_{32})$, $E(\text{Ti})$ and $E(\text{V})$ is the total energy of a $2\times 2\times 1$ supercell of pure anatase TiO_2 , the bulk hcp Ti and bcc V, respectively. E_s is predicted to be 2.34 eV, which is even less than one third of the substitution energy of Co dopant (8.51 eV).[8] This result agrees nicely with experimental observation that V impurity is well dissolved into TiO_2 . [13]

The band structure, total density of states (DOS) and V $3d$ partial DOS (PDOS) of $\text{Ti}_{15}\text{VO}_{32}$ are presented in Fig.2. The calculation at GGA level suggests that the DOS near the Fermi surface (E_F) mainly originates from V t_{2g} orbitals, which is shown in Fig.2(c) for clarity. The V impurity band has strong anisotropic character in the a - b plane (i.e. $A\rightarrow R$ and $\Gamma\rightarrow M$), however, it is less dispersive along the c axis of the BZ (i.e. $M\rightarrow A$ and $Z\rightarrow\Gamma$). It is important to note that E_F is largely crossed by spin-up states, while spin-down states only cut E_F slightly. This indicates that the system is nearly half-metallic at GGA level. As there exists strongly correlated interaction in V $3d$ shells, we choose DFT+U as a scheme beyond-GGA level. The calculated PDOS by DFT+U are plotted in Figs.2(e) and 2(f). We find that the metal-insulator-transition occurs when the parameter U is applied to the V atom. This strong correlation lifts the degeneracy of t_{2g} states, so as to open the gap. An occupied band composed of mainly d_{xy} component is split off from the bottom of the conduction band. These features suggest that Hubbard U correction increases the localization of the V d electrons. Results presented above are fundamentally consistent with Ref.[14] except for their lifted Ti PDOS due to additional corrections for Ti $3d$ states.

It can be expected that the direct impurity interaction can not yield experimentally observed strong FM because of the large V-V distance. The original supercell is extended

along b and c axis to form $2 \times 4 \times 1$ and $2 \times 2 \times 2$ supercells ($\text{Ti}_{30}\text{V}_2\text{O}_{64}$) to examine magnetic ordering. From Table I, the calculated energy difference between the AFM and FM states (ΔE) is negative, which indicates that the ground state is AFM for both cases as expected. Moreover, the on-site Coulomb repulsion at V atom strengthens AFM with a small increase of magnetic moment. The AFM ground state is further confirmed by our calculation using hybrid B3LYP functional as implemented in CRYSTAL03 code.[20] To understand the experimental observed high T_C in V-doped TiO_2 , one has to search other origins to lead FM. In the rest of this paper, first we explore the effects of closely distributed V impurities esp. at high doping level, then oxygen vacancy on electronic and magnetic properties.

According to Janisch *et al.*'s suggestion,[2, 9] we have constructed three $\text{Ti}_{14}\text{V}_2\text{O}_{32}$ structures to model high impurity concentration (12.5%) of V- TiO_2 , where a second V atom occupies Ti_2 , Ti_3 or Ti_4 site in the $\text{Ti}_{15}\text{VO}_{32}$ supercell, named the chain, grid and nearest-neighbor (NN) configurations (the optimized V-V distance is 3.82, 5.39 and 3.06 Å), respectively. From Table I, ΔE is positive for all three cases within GGA approach and increases with V-V distance decreasing. We find that the energy of the NN configuration is the lowest, strongly favoring V-dopants clustering.

The DOS shapes have almost the same characteristic shapes among three configurations, hence, only the one for the nearest-neighbor one is presented in Fig.3. Similar to the Co- TiO_2 case,[9] when x increases from 6.25% to 12.5%, the total DOS, V $3d$ PDOS and magnetic moment of V cation change slightly. The DOS and PDOS by DFT+U are presented in Figs.3(b) and 3(d), which reveal that the system becomes semiconductor when the parameter U is applied. It is consistent with the poor conductivity observed in V- TiO_2 samples. The on-site U correction shifts d_{xy} state down to the middle gap, while at GGA level it is a mixture of three t_{2g} orbitals (d_{xy} , d_{yz} and d_{xz}) locating at E_F . The larger separation between the occupied and empty V $3d$ states, due to strong correlation, results in the decrease of the ΔE value and even the change of its sign for the chain and grid configurations in Table I. The remarkable observation in our work is the high fidelity of ΔE for the NN configuration. As it is extremely hard to choose the accurate value for U, this result is particularly valuable to highlight the important contribution of V-O-V NN configuration to yield FM state.

The reason for the weakened FM couplings within DFT+U could be sought in terms of the p - d hopping mechanism[19]. The V impurities interact with orbitals of the same symmetry and form a set of bonding-antibonding states. Within GGA approximation, FM

state has an energy gain through the partial occupancy of V t_{2g} states. The Hubbard U at V sites results in a fully occupied d_{xy} band. In a FM arrangement, both bonding and antibonding levels are filled, and there is no energy gain for this coupling. In the AFM arrangement, the bonding states are filled for both spin up and down channels, while the antibonding ones are empty. It implies that AFM is favored between adjacent V cations when correlation effect is taken into account. However, there exists a strong competition due to superexchange. It is well-known that superexchange may have a FM contribution for filled shells. Recently, Janisch *et al.* argue that short-range superexchange between 90° metal-anion-metal bond plays a significant role in transition metal doped anatase TiO_2 . [9] We believe the FM originates from the superexchange interaction with the V-O-V bond angle about 104.9° in the NN configuration.

As indicated by previous work [11, 12], the presence of oxygen vacancy (V_O) may influence the distribution of dopants. To study the impact of V_O , three cases are considered: (a) $\text{Ti}_{16}\text{O}_{31}$ with one oxygen atom removing from the $2 \times 2 \times 1$ supercell of TiO_2 ; (b) The basal oxygen (O_1) of V-contained octahedron is removed from $\text{Ti}_{15}\text{VO}_{32}$ and subsequently the oxygen deficient cell is doubly enlarged along b axis, named as the basal O_1 $2 \times 4 \times 1$ configuration; (c) V_O occupies the vertex site of V-incorporated octahedron (by removing O_2) and the original supercell is doubly extended along c axis, denoted as the vertex O_2 $2 \times 2 \times 2$ configuration. After removing an oxygen atom from the cation-contained octahedron, the original structure experiences a considerable distortion. Cations next to the V_O site are repelled away. The calculated total energies indicate that V_O prefers to stay close to V than near Ti.

Fig.4 shows the DOS results for the $\text{Ti}_{16}\text{O}_{31}$ and basal O_1 $2 \times 4 \times 1$ configurations. When an oxygen atom is removed, a nonmagnetic defect state (mainly from Ti cations near V_O) appears at the bottom of the conduction band. If a V atom occupies the cation site of the oxygen-deficient octahedron, V $3d$ states overlap in energy with the defect state which yields 0.11 e transferred from the defect state to the empty V $3d$ spin-up state enhancing spin polarization of V ion. It fits quite well with the physical picture proposed by Coey *et al.* that the hybridization between the defect state and magnetic dopants' states will promote FM. [21] However, the V_O mediated magnetic coupling is sensitive to distance. [22] The polarons induced by V_O tend to parallelize their spins, corresponding to a ferromagnetic arrangement, only when their distance is less than a critical value, which is the case in the

basal O_1 $2 \times 4 \times 1$ configuration. When their distance increases larger than this critical value, the strict spin alignment between polarons disappeared. This leads to a loss of long-range coherence, as in the vertex O_2 $2 \times 2 \times 2$ case. Further efforts are needed to determine the exact critical distance required for polaron percolation in this system. DFT+U calculations qualitatively do not change the result given by GGA.

In summary, we have studied the structural, electronic and magnetic properties of V-doped anatase TiO_2 by both GGA and DFT+U calculations. The correlation effect is not well represented by GGA, while DFT+U calculations give a better physical picture. The results suggest that direct exchange between well separated V ions cannot account for the observed FM in this system. The superexchange interaction is responsible for the stable FM between nearest-neighbor V cations. The long-range interactions between oxygen defects induced magnetic polarons are sensitive to their distance. Provided that a macroscopic ferromagnetic clusters appear by polarons overlapping, the system favors FM. Thus, a combination of the long-range polaron percolation and the short-range superexchange through nearest-neighbor V atoms could contribute to the high T_C FM in V-doped anatase TiO_2 .

We thank Y.Wang for helpful discussion. This work is partially supported by the National Natural Science Foundation of China under Grand Nos. 20303015, 10674121, 50121202 and 20533030, by the USTC-HP HPC project, and by the SCCAS and Shanghai Supercomputer Center.

-
- [1] Y. Matsumoto, M. Murakami, T. Shono, T. Hasegawa, T. Fukumura, M. Kawasaki, P. Ahmet, T. Chikyow, S. Koshihara, and H. Koinuma, *Science* **291**, 854 (2001).
 - [2] R. Janisch, P. Gopal, and N. A. Spaldin, *J. Phys.: Condens. Matter* **17**, R657 (2005).
 - [3] H. Toyosaki, T. Fukumura, Y. Yamada, and M. Kawasaki, *Appl. Phys. Lett.* **86**, 182503 (2005).
 - [4] T. Zhao, S. R. Shindo, S. B. Ogale, H. Zhang, T. Venkatesan, R. Ramesh, and S. Das Sarma, *Phys. Rev. Lett.* **94**, 126601 (2005).
 - [5] J. W. Quilty, A. Shibata, J. Y. Son, K. Takubo, T. Mizokawa, H. Toyosaki, T. Fukumura, and M. Kawasaki, *Phys. Rev. Lett.* **96**, 027202 (2006).
 - [6] P. A. Stampe, R. J. Kennedy, Y. Xin, and J. S. Parker, *J. Appl. Phys.* **93**, 7864 (2003).

- [7] D. H. Kim, J. S. Yang, Y. S. Kim, T. W. Noh, S. D. Bu, S.-I. Baik, Y.-W. Kim, Y. D. Park, S. J. Pearton, J.-Y. Kim, J.-H. Park, H.-J. Lin, C. T. Chen, and Y. J. Song, Phys. Rev. B **71**, 014440 (2005).
- [8] Z. X. Yang, G. Liu, and R. Q. Wu, Phys. Rev. B **67**, 060402 (2003).
- [9] R. Janisch and N. A. Spaldin, Phys. Rev. B **73**, 035201 (2006).
- [10] H. M. Weng, X. P. Yang, J. M. Dong, H. Mizuseki, M. Kawasaki, and Y. Kawazoe, Phys. Rev. B **69**, 125219 (2004).
- [11] L. A. Errico, M. Rentería, and M. Weissmann, Phys. Rev. B **72**, 184425 (2005).
- [12] S. Duhalde, M. F. Vignolo, F. Golmar, C. Chilotte, C. E. Rodríguez Torres, L. A. Errico, A. F. Cabrera, M. Rentería, F. H. Sánchez, and M. Weissmann Phys. Rev. B **72**, 161313 (2005).
- [13] N. H. Hong, J. Sakai, and A. Hassini, Appl. Phys. Lett. **84**, 2602 (2004).
- [14] Y. Wang and D. J. Doren, Solid State Commun. **136**, 142 (2005); Y. Wang, private communication.
- [15] P. E. Blochl, Phys. Rev. B **50**, 17953 (1994).
- [16] G. Kresse and J. Furthmuller, Phys. Rev. B **54**, 11169 (1996).
- [17] J. P. Perdew, K. Burke, and M. Ernzerhof, Phys. Rev. Lett. **77**, 3865 (1996).
- [18] H. J. Monkhorst and J. D. Pack, Phys. Rev. B **13**, 5188 (1976).
- [19] T. Chanier, M. Sargolzaei, I. Opahle, R. Hayn, and K. Koepernik, Phys. Rev. B **73**, 134418 (2006).
- [20] V.R. Saunders, R. Dovesi, C. Roetti, R. Orlando, C. M. Zicovich-Wilson, N.M. Harrison, K. Doll, B. Civalleri, I.J. Bush, Ph. D 'Arco, M. Llunell, *CRYSTAL2003* User's Manual (University of Torino, Torino, 2003). ΔE value using B3LYP hybrid functional is -5.2 and -3.3 meV/atom for $2 \times 4 \times 1$ and $2 \times 2 \times 2$ configurations ,respectively.
- [21] J. M. D. Coey, M. Venkatesan, and C. B. Fitzgerald, Nat. Mater **4**, 173 (2005).
- [22] M. J. Calderon and S. Das Sarma, cond-mat/0603182 (unpublished).

TABLE I: Calculated energy difference between the AFM and FM states ($\Delta E = E(\text{AFM}) - E(\text{FM})$), and the ground state magnetic moment (M) per V atom for various configurations at GGA level and at DFT+U level. The data inside the parentheses are obtained by DFT+U approach.

Unit cells	$\Delta E(\text{meV/atom})$	$M(\mu_B)$
Ti₃₀V₂O₆₄:		
$2 \times 2 \times 2$	-1.0 (-4.2) ± 0.71 (± 0.83)	
$2 \times 4 \times 1$	-8.0 (-12.7) ± 0.69 (± 0.80)	
Ti₁₄V₂O₃₂:		
chain	60.2 (-5.0)	0.84 (± 0.81)
grid	21.8 (-56.0)	0.77 (± 0.83)
nearest-neighbor	75.2 (14.5)	0.89 (0.91)
Ti₃₀V₂O₆₂:		
basal O ₁ $2 \times 4 \times 1$	18.5 (18.5)	1.14 (1.37)
vertex O ₂ $2 \times 2 \times 2$	-3.8 (-4.5) ± 0.97 (± 1.17)	

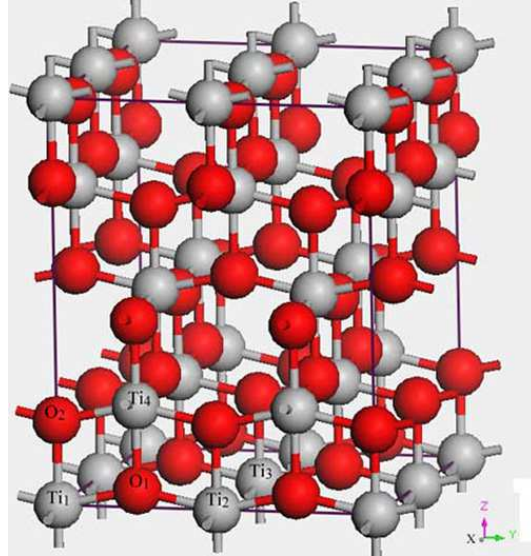


FIG. 1: (Color online) The schematic 48-atom supercell of anatase TiO_2 ($2 \times 2 \times 1$). The gray and red balls stand for Ti and O atoms, respectively.

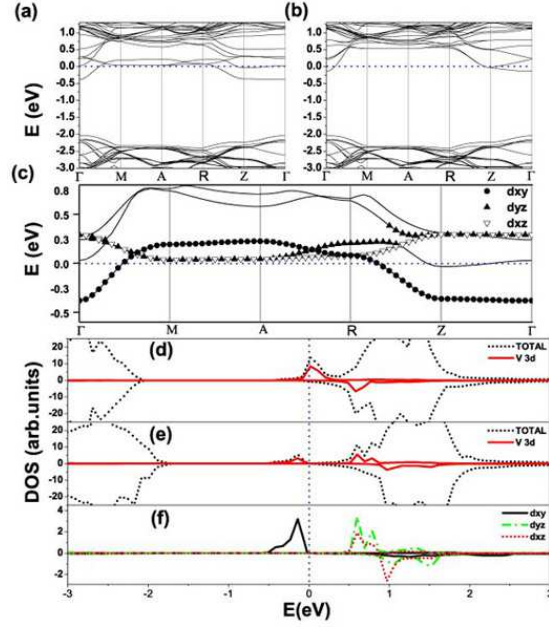


FIG. 2: (Color online) Band and DOS structure of V-doped anatase TiO_2 modeled by a $2 \times 2 \times 1$ supercell ($\text{Ti}_{15}\text{VO}_{32}$). (a),(b) the majority and minority spin GGA band structure. (c) majority spin around E_F . Total DOS and V 3d PDOS (d) GGA results, (e) DFT+U results. (f) DFT+U results of the projected DOS of V 3d orbitals. The Fermi energy is shifted to zero. $\Gamma=(0,0,0)$, $M=(1/2,1/2,0)$, $A=(1/2,1/2,1/2)$, $R=(1/2,0,1/2)$, and $Z=(0,0,1/2)$.

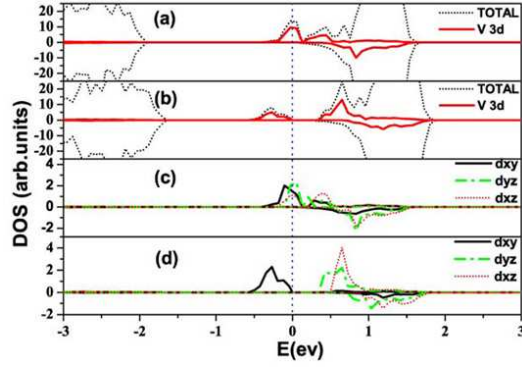


FIG. 3: (Color online) DOS structure of the nearest-neighbor configuration ($\text{Ti}_{14}\text{V}_2\text{O}_{32}$) with a ferromagnetic arrangement of the V moments. Total DOS and V 3d PDOS (a) GGA result, (b) DFT+U result. Projected DOS of V 3d orbitals (c) GGA result, (d) DFT+U result. The vertical line denotes the Fermi level.

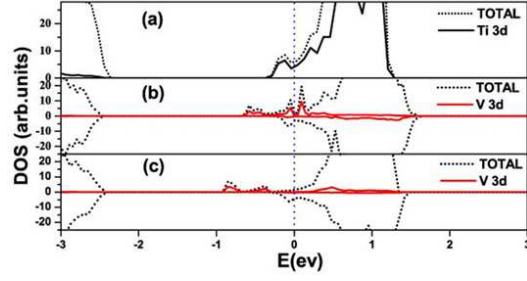


FIG. 4: (Color online) DOS structure of oxygen deficient $\text{Ti}_{16}\text{O}_{31}$ and the basal $\text{O}_1 2 \times 4 \times 1$ configuration ($\text{Ti}_{30}\text{V}_2\text{O}_{62}$). (a) Total DOS and $3d$ PDOS of Ti cations near the oxygen defect for $\text{Ti}_{16}\text{O}_{31}$. Total DOS and V $3d$ PDOS for the basal $\text{O}_1 2 \times 4 \times 1$ obtained within (b) GGA approach, (c) DFT+U method. The vertical line denotes the Fermi level.